Updating a Finite Element Based Structural Model of a Small Flexible Aircraft

Abhineet Gupta [*], Claudia P. Moreno[†], Harald Pfifer[‡], and Gary J. Balas[§]

Aerospace Engineering and Mechanics, University of Minnesota, Minneapolis, MN, 55455, USA

The generation of a finite element based structural model of a small, flexible unmanned aircraft is presented. The paper focuses on obtaining a simple model suitable for control design based on a two step procedure. In an initial step, static and dynamic tests of the wings are conducted. These experiments give first estimates of the material properties (e.g., stiffness) of the aircraft. A finite element model consisting of simple beam elements is constructed based on these first estimates. In the next step, the modal data of the aircraft is extracted from a ground vibration test. The initial finite element model is then updated using this modal data. An optimization problem is proposed to minimize the difference in the modal properties, i.e. the modal frequencies and mode shapes, between the model and the experimental data. The free parameters of the optimization are chosen based on physical insights of the system. The resulting finite element model closely matches the experimental data both in terms of modal properties as well as input/output behavior.

Nomenclature

δ_i	Heave of i^{th} node
θ_i	Bending of i^{th} node
ϕ_i	Twist of i^{th} node
E	Young's Modulus
G	Torsional Modulus
I	2^{nd} Moment of Inertia
J	Polar Moment of Inertia
n	Number of nodes considered
Φ_{id}	Mode Shape identified from experiment
Φ_{fe}	Mode Shape obtained from FE model
ω_{id}	Modal frequency identified from experiment
ω_{fe}	Modal frequency obtained from FE model
p	Parameters chosen for FE model update
μ	Mass per unit length
m_i	Point mass at ith point
$I_{xx(i)}$	Pitch inertia at ith point
$I_{zz(i)}$	Roll inertia at ith point

I. Introduction

Modern aircraft designers are adopting light-weight, high aspect ratio flexible wings to improve performance and reduce operation costs. However, the large deformation exhibited by these aircraft increase the interaction of the rigid body dynamics and structural vibration modes - usually the first wing bending mode.

[*]Graduate Research Assistant, Department of Aerospace Engineering and Mechanics, gupta165@umn.edu
[†]Graduate Research Assistant, Department of Aerospace Engineering and Mechanics, moren148@umn.edu
[‡]Postdoctoral Research Associate, Department of Aerospace Engineering and Mechanics, hpfifer@umn.edu
[§]Professor, Department of Aerospace Engineering and Mechanics, and AIAA Member, balas@umn.edu

This interaction, called body freedom flutter, leads to poor handling qualities and may result in dynamic instability. Hence, accurate models are required to predict and control this dangerous phenomenon.

Flutter analysis of aircraft has been widely studied in the literature[1–4] and numerous researchers have addressed aeroelastic modeling for highly flexible aircraft.[5–7] Currently, modeling aeroelastic behavior of flexible aircraft requires the development of a structural model coupled with an aerodynamic model. The nonlinear aeroelastic models are derived based on structural finite elements (FE) and lifting surface theory, both of which are available in general purpose commercial code.[8–10] However, accurate flutter prediction is highly dependent on the accuracy of these aerodynamic and structural models.

It is standard practice to improve the accuracy of structural models by updating the parameters in the finite element model using experimental modal data, see Section II. Various approaches for model updating exist in literature[11] which can be broadly categorized in two classes: Representational methods and knowledge based methods. In representational methods, the entries of the mass and/or stiffness matrix are directly updated. The optimization problem, in general, is to keep the mass and stiffness matrix in some metric close to the initial matrices while matching the experimental modal data. The advantage of this approach is that it can be solved analytically. However, since the entries of the mass and stiffness matrix are changed directly the connection to physical properties like inertias or Young's modulus is lost. Thus, representational methods only represent the actual structure in term of measured data. Knowledge based methods minimize the mismatch of the modal data between the FE model and the experiment. The free parameters of the optimization are chosen based on the knowledge of the structure and physical considerations, e.g. inertias or mass distribution. While these methods do not guarantee an exact match of the modal data, they keep the physical connection. Thus, physical insights can be drawn from the structural model which can prove to be invaluable to understand aeroelastic phenomena. For this reason the latter approach is pursued in this paper.

This paper presents an updating approach applied to a highly flexible unmanned aerial vehicle (UAV). The considered UAV, known as Body Freedom Flutter (BFF) aircraft, was developed by Lockheed Martin and Air Force Research Laboratory and is used by the Unmanned Aerial Vehicle Laboratories at University of Minnesota to carry out research on aeroservoelastic controls.[12] An initial FE model of the BFF vehicle has been generated using experimental data from simple static and dynamic test (Section III). Static experiments give an estimate of the stiffness properties of the structure while dynamic experiments, along with the results from the static experiment, are used to get an estimate of the mass and inertia properties of the structure. In Ref. 13, a ground vibration test of the aircraft was conducted and natural frequencies, damping factors and mode shapes of the structure have been identified. This paper uses the modal data from Ref. 13 to update the initial FE model. To that end, an optimization problem in proposed in Section V. Physical insight of the model is used to select the free parameters in the optimization. The results show that the updated model closely matches the GVT data. It should be emphasized that the structural model will be integrated into an aeroelastic model of the BFF aircraft with the purpose of designing flutter suppression control. Hence, it is important to have a simple structural model available.

The UAV group at the University of Minnesota follows an open source philosophy. All the data and software related to the aeroelastic research, including the FE model and the algorithm for model updating, is available online at `http://www.aem.umn.edu/~AeroServoElastic/`. It is hoped that the data and the software would be a great resource for researchers in the field of aeroservoelastic analysis and controls.

II. Background

The objective of FE model updating is to obtain a mathematical model of the structural dynamics that closely matches experimental data. In this paper, a knowledge based approach is considered. In the approach the user chooses the parameters to be updated allowing to retain the physicality of the mathematical model. Typical choices of free parameters are mass distributions, inertias and material properties (e.g., Young's modulus). The disadvantage with this method is that the optimization problem is nonconvex and computationally expensive. It is still the preferred method, as the physicality allows more insights from the structural model which can prove to be very valuable for analyzing an aircraft and its aeroelastic behavior. The disadvantages of the methods, in general, come into effect especially with large, complex structural models. Since the paper focuses on simple models suitable for control design, a knowledge based approach can be applied with reasonable computational effort.

A wide variety of metrics are used in literature to quantify the distance between the experimental data

and the FE model.[14] Common choices are fitting the frequency response data or the modal properties, i.e. mode frequencies and shapes. The latter is chosen in the paper, as the ultimate purpose of the structural model is to be integrated into a full aeroelastic model of the aircraft. To this end, only the modal data and not the specific input/output behavior of the GVT is required. The difference in the frequencies is measured as a relative error. For n identified modes, the error vector can be written as

$$e_\omega(p) = \begin{bmatrix} \frac{\omega_{id,1}-\omega_{fe,1}(p)}{\omega_{id,1}} & \dots & \frac{\omega_{id,n}-\omega_{fe,n}(p)}{\omega_{id,n}} \end{bmatrix}^T, \tag{1}$$

where $\omega_{id,i}$ and $\omega_{fe,i}(p)$ are the frequencies of the i^{th} mode of the GVT and the FE model respectively. The latter depends on the vector p which represents the free parameters in the optimization. As metric for the mode shapes the so-called Modal Assurance Criteria (MAC) is used which is a standard metric in literature.[14,15] It is a scalar value that describes the linearity between two mode shapes. The MAC is defined by

$$\text{MAC}(\phi_{id,i}, \phi_{fe,i}) := \frac{|\phi_{id,i}^T \phi_{fe,i}|^2}{\phi_{id,i}^T \phi_{id,i} \phi_{fe,i}^T \phi_{fe,i}}, \tag{2}$$

where $\phi_{id,i}$ and $\phi_{fe,i}$ are the i^{th} modal vector of the GVT an FE model respectively. The MAC can take values between 0 and 1, where 1 means that the modal vectors are consistent and 0 that they are orthogonal.

In order to obtain the mode shapes from the experimental data, it is assumed that the GVT measures the response to the excitation at q points distributed across the structure. At each modal frequency of the n considered modes at each measurement location of the GVT data, the imaginary part of the frequency response function, also known as quadrature response, is extracted. The quadrature response can be written as a linear combination of the contribution of the different mode shapes.[16] The equation for the j^{th} mode at the k^{th} measurement point is given by

$$R_{\omega=\omega_j,k} = R_{j,k} + \sum_{i=1, i\neq j}^{n} \frac{(2\zeta_i)^2 \frac{\omega_{id,j}}{\omega_{id,i}}}{(1-(\frac{\omega_{id,j}}{\omega_{id,i}})^2)^2 + (2\zeta_i \frac{\omega_{id,j}}{\omega_{id,i}})^2} R_{i,k} \tag{3}$$

Here $R_{\omega=\omega_j}$ is the quadrature response for the k^{th} grid point and the j^{th} mode. $R_{i,k}$ is the contribution of i^{th} mode in the quadrature response and ζ_i is the modal damping for the i^{th} mode. At each measurement k this accounts for n equations in the n unknowns $R_{i,k}$ which can be readily solved. The values of the $R_{i,k}$ for all the points in the grid for a particular mode written in a vector represent the mode shape Φ_i for that particular mode.

Having the modal properties form experiments the following optimization problem is proposed to update a FE model:

$$\min_p \sum_{i=1}^{n} [1 - \text{MAC}(\Phi_{id,i}, \Phi_{fe,i}(p))] + \|e_\omega(p)\|] \tag{4}$$

The optimization tries to bring the MAC value for each mode shape closer to 1, while at the same time reduce the gap between the modal frequencies from the FE model and those calculated using experiments. It shall be noted that choosing the right parameters p is a difficult tasks and is highly problem dependent. In general, additional constraints are added to the optimization problem (4). Specifically, the parameters p are restricted to a physically meaningful domain or constraints on other physical parameters like total mass or center of gravity location are imposed.

III. Body Freedom Flutter Aircraft

The Body Freedom Flutter (BFF) aircraft was developed by Lockheed Martin and the Air Force Research Laboratory for demonstration of active flutter suppression technologies.[5] The aircraft was donated to the unmanned aerial vehicle (UAV) research group of the University of Minnesota to expand the research on aeroservoelasticity. However, limited information was provided with the BFF transfer, making the modeling of this aeroservoelastic vehicle even more challenging. The BFF aircraft is a high-aspect-ratio flying wing with lightweight airfoil made from a rigid center body and foam core flexible wings. The mass properties of the aircraft were obtained from experiments reported by Ref. 7. The estimates of inertia and center of gravity are summarized in the Table 1. Note that these values are only estimates based on experiments.

Table 1. Specifications of BFF aircraft

Property	Value
Total Mass	5.42 kg
CG location (from nose)	0.59 m
Roll Inertia	2.50 kg-m^2
Pitch Inertia	0.36 kg-m^2

Specifically, the roll inertia was reported to be difficult to measure, so that a high level of uncertainty is assumed in the given value.

The system identification of the structural dynamics of the BFF aircraft was presented by Moreno et al.[13] This paper identified the modal parameters of the flexible structure by performing a ground vibration test (GVT). The aircraft was excited with a sine sweep wave from 3 to 35 Hz and acceleration responses from 34 points distributed along the wing and center body of the vehicle are measured. Figure 1 depicts these point locations in the aircraft. Point 12 was selected to apply the excitation the structure.

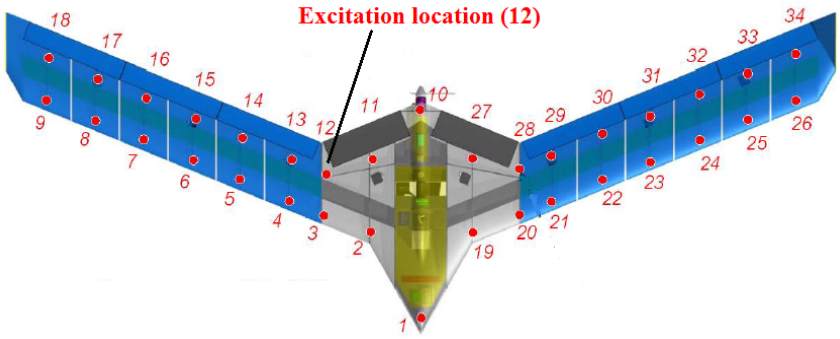

Figure 1. Input and output measurement locations[12]

Single input, single output (SISO) frequency responses from applied force to acceleration response at each location were obtained using a dynamic analyzer. A single input, multiple output (SIMO) state-space systems with 12 states was estimated for all experimental frequency responses and 6 flexible modes were identified in the excited frequency range. The results for natural frequencies and modal damping for the identified modes are summarized in table 2. Figure 2 sketches the mode shapes associated to each natural frequency of the aircraft. Here, the relative accelerations from the 34 measurement points are used to plot the pattern of motion.

Table 2. Natural frequencies, damping factors and modal shapes

Mode Shape	Identified Data	
	Freq [Hz]	Damp [%]
Sym 1st Bending	5.67	1.55
A/S 1st Bending	8.37	1.06
Sym 1st Torsion	18.34	2.06
A/S 1st Torsion	19.82	2.33
Sym 2nd Bending	23.17	2.85
A/S 2nd Bending	28.60	2.55

IV. Finite Element Model

Several element properties can be used to model a structure according to the application. One-dimensional elements with axial, bending and torsional properties are generally used to model trusses, beams or frames.

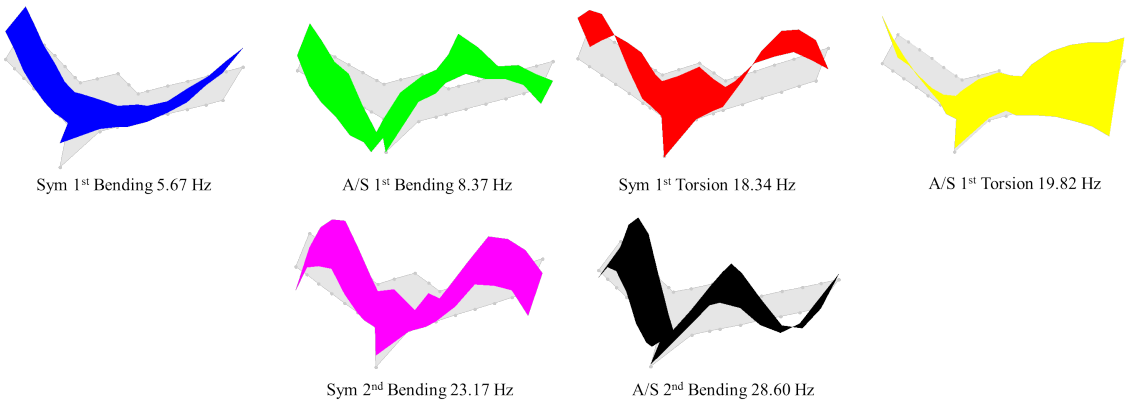

Figure 2. Identified mode shapes

These elements usually have two nodes, one at each end, and are located at the centroidal axis of the real elements. Simple structural models of light-weight aircraft can be modeled with one-dimensional elements. A typical element used for this application is the Bernoulli beam with torsional effects, which represents the main load case of the aircraft in flight. Fig. 3 shows the degrees-of-freedom (DOF) considered in this typical beam element. The element mass and stiffness matrices are presented in Eq. (5) and Eq. (6) respectively.[20]

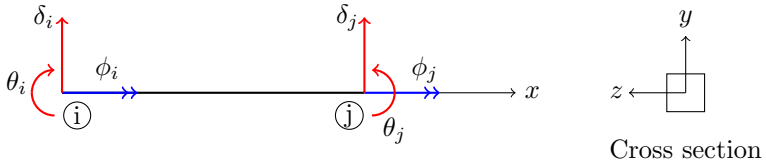

Figure 3. Beam element

$$m_e = \begin{array}{c} \begin{matrix} \delta_i & \theta_i & \phi_i & \delta_j & \theta_j & \phi_j \end{matrix} \\ \begin{pmatrix} \frac{156\mu L}{420} & \frac{22\mu L^2}{420} & 0 & \frac{54\mu L}{420} & \frac{-13\mu L^2}{420} & 0 \\ \frac{22\mu L^2}{420} & \frac{4\mu L^3}{420} & 0 & \frac{13\mu L^2}{420} & \frac{3\mu L^3}{420} & 0 \\ 0 & 0 & \frac{\chi L}{3} & 0 & 0 & \frac{\chi L}{6} \\ \frac{54\mu L}{420} & \frac{13\mu L^2}{420} & 0 & \frac{156\mu L}{420} & \frac{-22\mu L^2}{420} & 0 \\ \frac{-13\mu L^2}{420} & \frac{-3\mu L^3}{420} & 0 & \frac{-22\mu L^2}{420} & \frac{4\mu L^3}{420} & 0 \\ 0 & 0 & \frac{\chi L}{6} & 0 & 0 & \frac{\chi L}{3} \end{pmatrix} \end{array} \tag{5}$$

$$k_e = \begin{array}{c} \begin{matrix} \delta_i & \theta_i & \phi_i & \delta_j & \theta_j & \phi_j \end{matrix} \\ \begin{pmatrix} \frac{12EI_z}{L^3} & \frac{6EI_z}{L^2} & 0 & \frac{-12EI_z}{L^3} & \frac{6EI_z}{L^2} & 0 \\ \frac{6EI_z}{L^2} & \frac{4EI_z}{L} & 0 & \frac{-6EI_z}{L^2} & \frac{2EI_z}{L} & 0 \\ 0 & 0 & \frac{GJ_x}{L} & 0 & 0 & \frac{-GJ_x}{L} \\ \frac{-12EI_z}{L^3} & \frac{-6EI_z}{L^2} & 0 & \frac{12EI_z}{L^3} & \frac{-6EI_z}{L^2} & 0 \\ \frac{6EI_z}{L^2} & \frac{2EI_z}{L} & 0 & \frac{-6EI_z}{L^2} & \frac{4EI_z}{L} & 0 \\ 0 & 0 & \frac{-GJ_x}{L} & 0 & 0 & \frac{GJ_x}{L} \end{pmatrix} \end{array} \tag{6}$$

Here, EI_z represents the bending stiffness around the z-axis, GJ_x the torsional stiffness, and L the length of the element. The elastic and material properties of the elements are represented by the Young modulus E, shear modulus G, section mass per unit length μ, and inertia per unit length χ. Cross section properties are the second area moment around the z-axis, I_z, and the polar moment of inertia around the x-axis, J_x.

The structure of the BFF vehicle is modeled as a free beam that represents the wing spars and center body of the aircraft (Fig. 4). The structure is discretized based on the physical characteristics of the BFF such as actuators, winglets and electronics location. The fuselage is assumed rigid and modeled with equivalent

beams between nodes 9-1-4 and rigid connections between point masses that represent the electronics and accessories in the aircraft. Node 1 represents the center of gravity of the aircraft, node 2 the propulsion motor and node 3 the flight computer locations. The length of each wing (nodes 4-8 and 9-13) is taken as 1.27 m with a sweep angle of 22 deg. The wing is discretized in 4 elements to take into account the point masses of the actuators corresponding to inboard flaps (5,10), mid-board flaps (6,11) and outboard flaps (7,12). The winglets are located at nodes 8 and 13. Lastly, additional rigid elements connecting some of the experimental points are modeled in order to easily compare frequency response data. Here, node 17 represents the experimental excitation point.

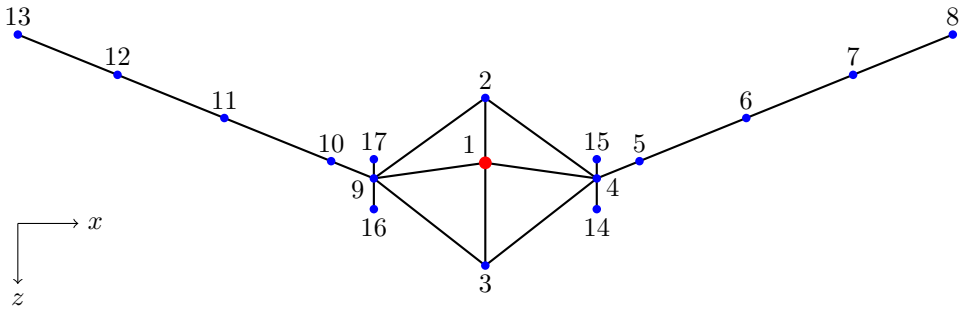

Figure 4. FE based structural model of BFF

Because detailed structural information was not provided with the aircraft, additional experiments are needed to obtain the static and dynamic properties of the wing elements. The following subsections describe the main results used to build the FE model for the BFF vehicle.

Wing Static Tests

Static tests are conducted just on the wings of the aircraft to obtain initial estimates of the stiffness properties of the wings. The setup is shown in Fig. 5. The BFF aircraft wing is fixed with clamps at 1.15 m from the tip of the wing. An inclinometer that measures the angular deflection in two directions is located at 1 m from the fixed end. Three weights were applied at two different locations along the wing, $l_1 = 0.9$ m and $l_2 = 0.6$ m from the fixed end. Measurements for bending and torsion deflections are taken by applying eccentric loads at 10 cm from the elastic axis of the wing. Analysis of the data resulted in a bending stiffness $EI_z = 70\,\text{N-m}^2$ and torsion stiffness $GJ_x = 40\,\text{N-m}^2$.

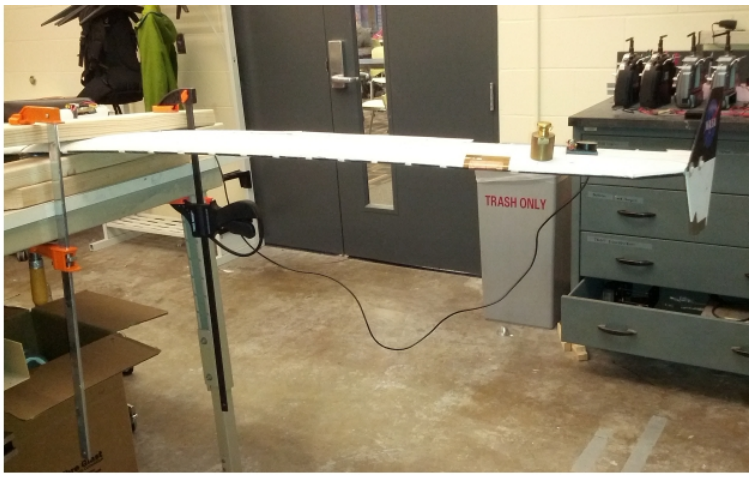

Figure 5. Static test setup

Wing Dynamic Tests

An estimation of the wing mass properties is obtained from dynamic tests. As in the static test, the aircraft wing is fixed with clamps at 1.15 m from the tip of the wing. Accelerometers are located in the tip of the wing in the elastic axis and at 10 cm from the elastic axis. Initial displacements are applied to the tip of the wing and time histories of the free vibration are obtained. Power spectra of the acceleration data is computed to identify the frequency content of the wing dynamics. Fig. 6 shows the power spectrum for one of the free vibration records corresponding to the eccentric accelerometer. Two bending frequencies at $f_1 = 3.37\,\text{Hz}$, $f_3 = 24\,\text{Hz}$ and one torsion frequency at $f_2 = 18.6\,\text{Hz}$ are identified. Assuming the wing as a cantilever beam with fundamental bending frequency, $\omega_b = (0.597\pi/L)^2\sqrt{EI_z/\mu}$ and fundamental torsional frequency, $\omega_t = (\pi/2L)\sqrt{GJ_x/\chi}$ in rad/s, the mass distribution and inertia of the wing are found to be $\mu = 1.0797\,\text{kg/m}$ and $\chi = 0.0054\,\text{kg-m}^2/\text{m}$.

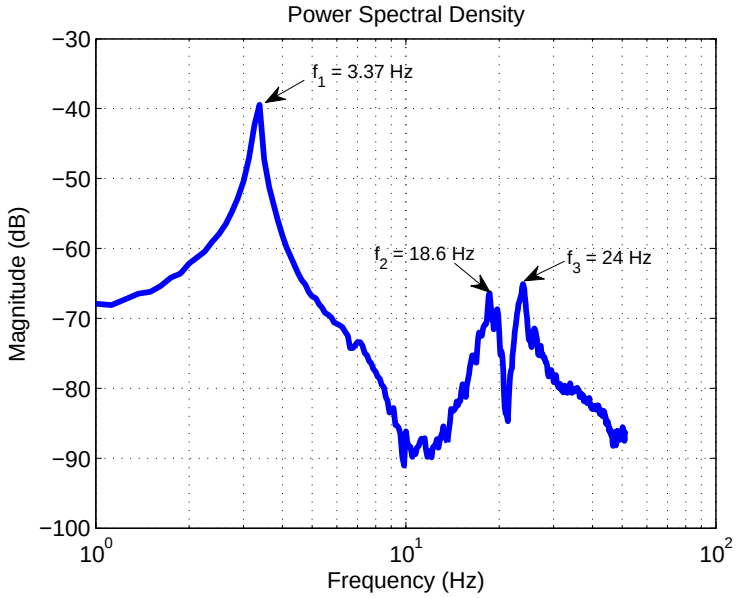

Figure 6. Power spectrum of the BFF wing free vibration for eccentric accelerometer

Based on the dimensions of the wing spar and the stiffness properties estimated, the elastic properties of the wing are obtained. The rectangular cross section of the spar measured is equivalent to $b = 7.62\,\text{cm}$ width and $h = 0.65\,\text{cm}$ height. Hence, the corresponding Young's modulus is computed as $E = 40.14\,\text{GPa}$ and shear modulus as $G = 16.57\,\text{MPa}$. Stiffness values for the center body elements, considered rigid, are about 6 order of magnitude higher than wing stiffness properties.

Point masses to represent actuators, batteries and electronics are added to the model. As these electronic elements are located inside the aircraft structure, they can not be measured directly. Hence, estimates of their weights are used for the initial FE model. Actuators for the body and outboard flaps weigh approximately 65 g, actuators for the inboard and middle flaps weigh 50 g, winglets are 50 g, batteries 2.25 kg, propulsion motor 200 g and electronics 150 g. Lastly, additional inertia is located at the center of gravity to account for the use of lumped masses and match the total aircraft inertia which has been obtained from swing tests in Ref. 7.

Table 3 shows the natural frequencies computed using the assembled mass and stiffness matrices of the structure and compares these results with the identified frequencies from the GVT. It can be seen that non of the modal frequencies and mode shape combination is satisfactory. The low value of some of the MAC values suggests that some of the modes might have been switched in order. This hypothesis is confirmed by the non diagonal nature of the MAC matrix as shown in Fig. 7. Hence, parameter updating is required to obtain a more accurate FE model.

Table 3. Natural frequencies: Initial Finite element (FE) model vs. Ground vibration test (GVT)

Mode Shape	Initial FE Model Freq [Hz]	GVT Freq [Hz]	MAC Value
Sym 1st Bending	3.96	5.67	0.74
A/S 1st Bending	6.00	8.37	0.87
Sym 1st Torsion	18.15	18.34	0.52
A/S 1st Torsion	20.47	19.82	0.02
Sym 2nd Bending	27.83	23.17	0.06
A/S 2nd Bending	28.16	28.60	0.01

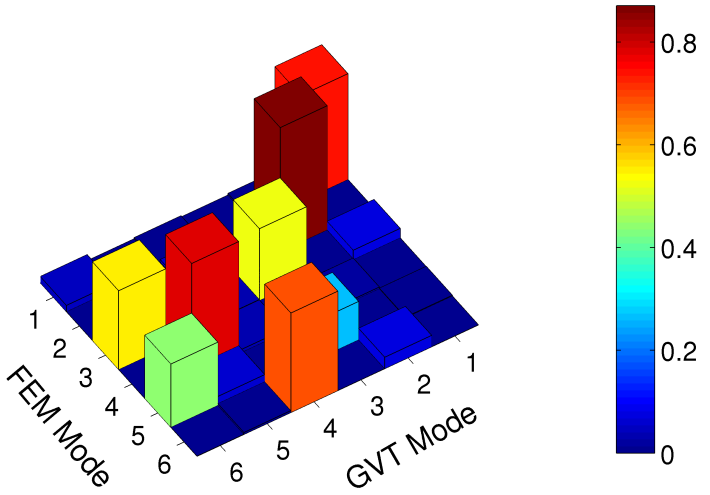

Figure 7. MAC between different modes: Initial FE model

V. Model Updating

The FE model of the BFF aircraft needs to be updated to better represent the measured data. Selecting the parameters to update is a crucial step in the model validation and considerable thoughts should be given to it. In this paper, three aspects are considered for selecting the updating parameters when using iterative methods: physical meaning, uniqueness and identifiability.[23] Because the finite element model is based on physical properties, variation of mass and stiffness parameters should be constrained such that physical meaning remains intact. On the other hand, setting physical constraints will also impose uniqueness to the solution because many different sets of parameters could result in similar model outputs. Finally, the ability to identify what parameters can or can not be measured with sufficient confidence is perhaps the most important step in the model updating process.

V.A. Parameter Selection: Allowable Variation and Constraints

Based on these considerations, the mass and stiffness element definition and the wing experiments performed, the set of parameters chosen to vary in a certain interval are the mass distribution for both wings and fuselage, additional point masses and inertia, and the elastic modulus of the wing material. Geometric properties, such as beam cross section dimensions and element lengths, are fixed for the BFF aircraft. The reason to choose these parameters is that the mass distribution of the aircraft is not perfectly known. Information about weight and location of internal elements (e.g. wiring, sensors) are not known by the University of Minnesota. Similar situation is encountered by the material composition and mechanical properties of the elements, which were estimated by the simple tests described in the previous section.

Table 4 shows the interval variation allowed for the parameters selected as well as their initial value.

Here, the Young's modulus and shear modulus for the wings (E_{wing} and G_{wing}) are restricted to a relative small interval around the initial estimates because the static tests performed are assumed fairly accurate. Given the poor knowledge of the aircraft mass distribution, specially in the center body, the point masses at the center of gravity m_1 and the mass per unit length, $\mu_{fuselage}$ are allowed to vary significantly from their initial value. The other point masses in the fuselage (m_2, m_3) are also allowed to vary from zero up to 3 times their initial estimate. However, an inverse relation between the distributed and lumped mass is constraining the problem from adding excessive weight to the fuselage or wings, i.e. if the mass per unit length increases the additional point mass will decrease. Similarly the distributed mass in the wings μ_{wing} is allowed to vary in a large interval. Lastly, additional local masses and inertias are added to the wing nodes (4-13) . As mentioned previously, the aircraft roll inertia value obtained from experiments has poor accuracy, hence, variations in the roll inertia of each node are allowed in both wings and center of gravity. Because the aircraft pitch inertia was estimated with good accuracy, only a small variation of this parameter value is allowed at the center of gravity. Lastly, general aircraft physical constraints are added to the model updating problem. Recall that the total mass of the aircraft was measured as 5.42 ± 0.2 kg, the center of gravity 0.59 ± 0.05 m and the pitch inertia 0.36 ± 0.04 kg-m^2.

Table 4. Parameters of the FEM model

Parameter	Estimated Value	Optimization Interval	
		Lower Bound	Upper Bound
$\mu_{fuselage}$	0.01 Kg/m	0.3 Kg/m	1.4 Kg/m
E_{wing}	40.14 GPa	35 GPa	75 GPa
G_{wing}	24.23 MPa	5 MPa	25 MPa
μ_{wing}	1.08 Kg/m	0.1 Kg/m	1.2 Kg/m
m_1	2.25 Kg	0.0 Kg	2.25 Kg
m_2	0.15 Kg	0.0 Kg	0.6 Kg
m_3	0.20 Kg	0.0 Kg	0.6 Kg
$m_{4,9}$	0.065 Kg	0.0 Kg	0.2 Kg
$m_{5,10}$	0.02 Kg	0.0 Kg	0.2 Kg
$m_{6,11}$	0.02 Kg	0.0 Kg	0.2 Kg
$m_{7,12}$	0.065 Kg	0.0 Kg	0.2 Kg
$m_{8,13}$	0.05 Kg	0.0 Kg	0.2 Kg
Iz_1	0.3 Kg-m^2	0.0 Kg-m^2	1.0 Kg-m^2
Ix_1	0.18 Kg-m^2	0.0 Kg-m^2	0.2 Kg-m^2
$Ix_{4,9}$	0.0008 Kg-m^2	0.0 Kg-m^2	0.01 Kg-m^2
$Ix_{5,10}$	0.0008 Kg-m^2	0.0 Kg-m^2	0.01 Kg-m^2
$Ix_{6,11}$	0.0008 Kg-m^2	0.0 Kg-m^2	0.01 Kg-m^2
$Ix_{7,12}$	0.0008 Kg-m^2	0.0 Kg-m^2	0.01 Kg-m^2
$Ix_{8,13}$	0.0008 Kg-m^2	0.0 Kg-m^2	0.01 Kg-m^2

V.B. Optimization Problem

The minimization introduced in Section II is used to update the FE model. The free parameters p are chosen according to Table 4 section and the additional constraints given above are included in the problem. The first six modes identified in Ref.[13] are included in the cost function. An evolutionary algorithm known as differential evolution[25] is used to solve the problem. Differential evolution is well suited for nonconvex optimizations and is known for its quick convergence rate.[24] The optimization was run for 100 iteration with 200 population members for an hour. The value of the cost function decreased from 0.353 to 0.058.

The solution of the optimization problem give the updated values of the parameters of the FE model. The optimum values of the parameters are shown in table 5. It can be seen the optimized value of average mass per unit length for the wing, which is a combination of μ_{wing} and the point masses, comes out to 1.02 which is very close to the estimated value of 1.08. Similarly, the optimized value of average inertia

of the wings, which includes contribution from both point inertias and distributed inertia, is calculated as 0.0079 as compared to 0.0053 from the experiments. The Young's modulus and torsional modulus have changed considerably from 40.1 GPa to 56 GPa and from 14.2 MPa to 23.4 Mpa. The point mass at the CG has decreased and the distributed mass in the fuselage has increased which represents the correct mass distribution in the fuselage.

These parameters are substituted back into the FE model to obtain the final structural model of the aircraft. The modal frequencies and mode shapes are calculated from the FE model. This data is compared with the identified modal data in table 6. It can be seen that the update process is able to identify the modal frequencies quite close to the identified frequencies for all the modes. Although, the 1^{st} symmetric torsion frequency is still not as close to the identified frequency as other frequencies are. The mode shapes from the updated FE model are also close to the identified mode shapes as the six mode shapes considered have MAC values of over 0.8 between the updated and identified mode shapes. The MAC between different mode shapes from the FE model and from the experiments are plotted in figure 8. It can be seen that the MAC matrix is diagonal and thus, it can be concluded that the modes appear in the same order as observed in the GVT. Also, the final value of the mass properties of the aircraft are shown in table 7. All the quantities except for roll inertia had strict constraints on them. The FE model predicts the roll inertia to be 2.858 Kg-m^2 which is close to the estimate of 2.5 Kg-m^2. Mode shapes of the first 6 modes are also plotted and shown in figure 9 and figure 10. The frequency response function between one of the points (Point 15) on the right wing trailing edge and the excitation point (Point 12) is plotted in figure 11 for both initial FE model and final model and are compared with the corresponding result from the experiments. It can be seen that the frequency response function of the updated FE model is quite close to that obtained from GVT. The same trend is observed for all the points on the aircraft.

Table 5. Optimized values of the FE parameters

Parameter	Optimized Value
$\mu_{fuselage}$	0.60 Kg/m
E_{wing}	56 Gpa
G_{wing}	23.4 Mpa
μ_{wing}	0.62 Kg.m
m_1	0.10 Kg
m_2	0.0 Kg
m_3	0.60 Kg
$m_{4,9}$	0.20 Kg
$m_{5,10}$	0.0 Kg
$m_{6,11}$	0.14 Kg
$m_{7,12}$	0.19 Kg
$m_{8,13}$	0.08 Kg
Iz_1	0.0 Kg-m^2
Ix_1	0.06 Kg-m^2
$Ix_{4,9}$	0.0 Kg-m^2
$Ix_{5,10}$	0.006 Kg-m^2
$Ix_{6,11}$	0.0 Kg-m^2
$Ix_{7,12}$	0.002 Kg-m^2
$Ix_{8,13}$	0.002 Kg-m^2

VI. Conclusion

An Euler Bernoulli Beam element based finite element model of the structural dynamics of BFF aircraft is created. Estimates of the mass and stiffness properties of the aircraft structure, which are obtained by conducting simple static and dynamic tests, are used to create an initial FE model. GVT is conducted to

Table 6. Comparison between experimental and updated FE modal data

Mode	Frequency		MAC(Φ_{id}, Φ_{fe})
	GVT	FE	
1^{st} Symmetric Bending	5.63	5.53	0.83
1^{st} Anti-Symmetric Bending	8.38	8.58	0.92
1^{st} Symmetric Torsion	18.44	19.21	0.84
1^{st} Anti-Symmetric Torsion	19.81	19.88	0.93
2^{nd} Symmetric Bending	23.07	23.03	0.93
2^{nd} Anti-Symmetric Bending	28.59	27.54	0.92

Table 7. Mass properties of the updated FEM model

Property	Value from FEM model
Centre of Gravity Location	0.61 m
Total Mass	5.381 Kg
Pitch Inertia	0.341 Kg-m^2
Roll Inertia	2.858 Kg-m^2

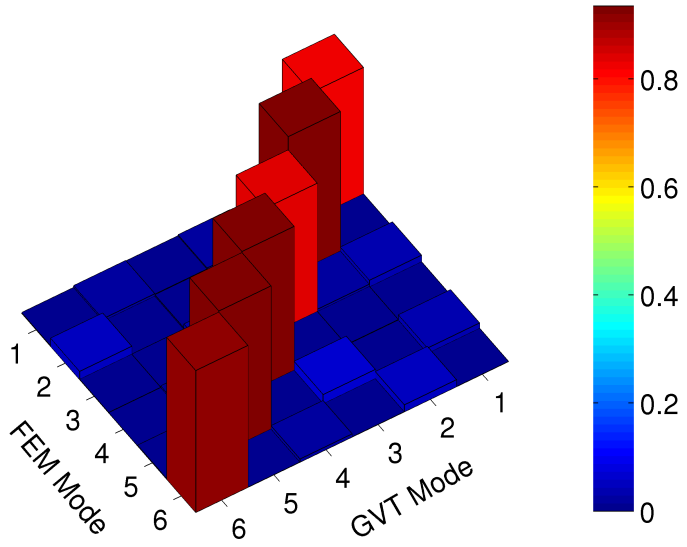

Figure 8. MAC between different modes

obtain modal data of the aircraft. The initial FE model is parameterized and the optimum value of those parameters are found by minimizing a cost function which represents the gap between the two modal data. The optimum set of parameters are substituted back into the FE model to obtain the final structural model of the aircraft. The final FE model is available online at `http://www.aem.umn.edu/~AeroServoElastic/`, along with all the data and software used for aeroelastic research in the UAV group in University of Minnesota.

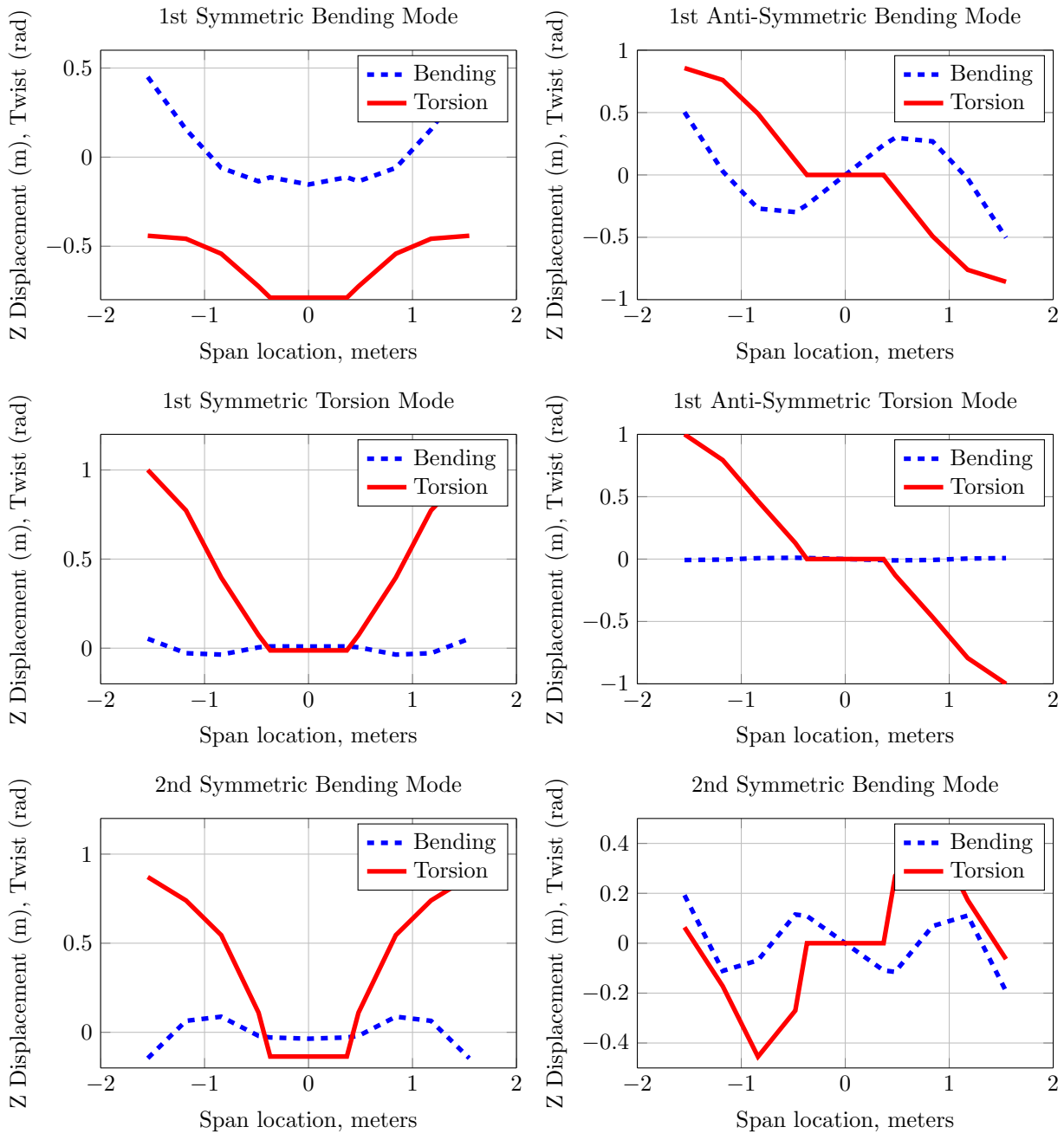

Figure 9. Mode shapes from optimized FE model

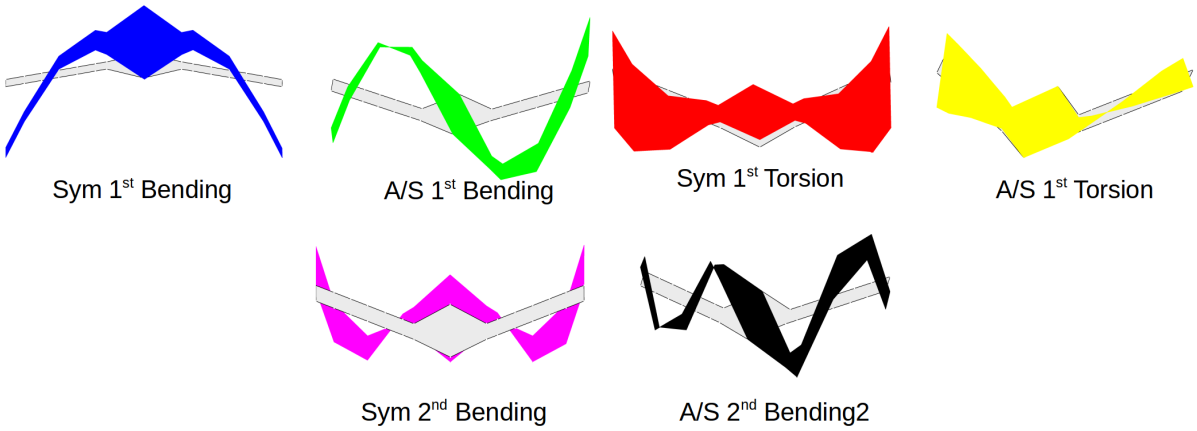

Figure 10. Mode shapes from optimized FE model

Frequency Response Function comparison for point 15 on GVT gird

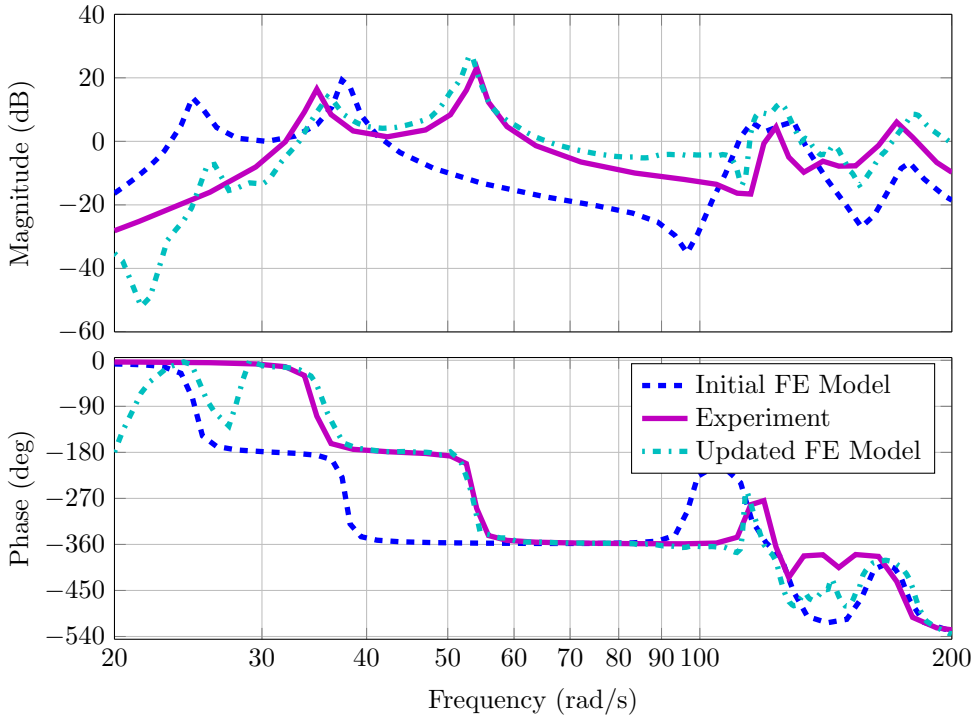

Figure 11. Frequency Response Function comparison

References

[1]Lind, R., and Brenner, M., *Robust Aeroservoelastic Stability Analysis*, Springer-Verlag, London, 1999.

[2]Benani, S., Van Staveren, J. W., Beuker, B., and Meijer, J. J., "Flutter analysis of an F-16A/B in heavy store configuration", *Journal of Aircraft*, Vol. 42, No. 6, 2005, pp. 1565-1574.

[3]Lind, R., "Flutter margins for multimode unstable couplings with associated flutter confidence", *Journal of Aircraft*, Vol. 46, No. 5, 2009, pp. 1563-1568.

[4]Baldelli, D. H., Zeng, J., Lind, R., and Harris, C., "Flutter-Prediction tool for flight-test-based aeroelastic parameter-varying models", *Journal of Guidance, Control and Dynamic*, Vol. 32, No. 1, 2009, pp. 158-171.

[5]Beranek, J., Nicolai, L., Buonanno, M., Burnett, E., Atkinson, C., Holm-Hansen, B. and Flick, P., Conceptual design of a multiutility aeroelastic demonstrator, *13th AIAA/ISSMO Multidisciplinary Analysis Optimization Conference*, Fort Worth, TX, 2010, pp. 2194- 2208.

[6]Waszak, M. R., Schmidt, D. K., "Flight dynamics of aeroelastic vehicles", *Journal of Aircraft*, Vol. 25, 1988, pp. 563-571.

[7]Kotikalpudi, A., and C. Moreno, B. Taylor, H. Pfifer and G. Balas, "Low Cost Development of a Nonlinear Simulation for a Flexible Uninhabited Air Vehicle, " American Control Conference, pp. 2029-2034, 2014.

[8]*MSC/NASTRAN, Structural and Multidiscipline Finite Element Analysis*, Software Package, Ver. 2012, MSC Software Corporation, Santa Ana, CA, 2012.

[9]*FEMAP, Engineering Finite Element Analysis, Software Package*, Ver. 10.3, Siemens PLM Software, Munich, Germany, 2012.

[10]*ZAERO, Engineers Toolkit for Aeroelastic Solutions, Software Package*, Ver. 8.5, ZONA Technology Inc., Scottsdale, AZ, 2011.

[11]Mottershead, J. E., and Friswell, M. I., "Model updating in structural dynamics: A survey", *Journal of Sound and Vibration*, 176(2), 1993, pp.347-375.

[12]Burnett, E., Atkinson, C., Beranek, J., Sibbitt, B., Holm-Hansen, B., and Nicolai, L., "NDOF Simulation model for flight control development with flight test correlation", *AIAA Modeling and Simulation Technologies Conference*, Toronto, Canada, 2010, pp. 7780-7794.

[13]Moreno, C. P., Gupta, A., Pfifer, H., Taylor, B., and Balas, G. J., "Structural Model Identification of a Small Flexible Aircraft", *2014 American Control Conference*, Portland, Oregon, USA, June 2014.

[14]Zienkiewichz, O. C., and Taylor, R. L., *The Finite Element Method for Solid and Structural Mechanics*, Elsevier Limited, 2005

[15]Boris, A. Z., and Juan, M. C., "Finite element model updating: multiple alternatives", *Engineering Structures*, Vol. 30, 2008, pp. 3724-3730.

[16]Stahle, C. V., and Forlifer, W. R., "Ground Vibration Testing of Complex Structure", *Flight Flutter Testing Symposium*, 1958, pp. 83-90.

[17]Caesar, B., and Peter, J., "Direct update of mathematical models from modal test data", AIAA Journal, Vol. 25, No. 11, 1987, pp. 1494-1499, 2014.

[18]Allemang, R. J., and Brown, D. L., "A correlation coefficient for modal vector analysis", *1st International Modal Analysis Conference*, Orlando, Florida, 1982, pp. 110-116.

[19]"UAV Research Group", University of Minnesota, *https://www.uav.aem.umn.edu*.

[20]Gunakala, S. R., Comissiong, D. M. G., Jordan, K., and Sankar, A, "A finite element solution of beam equation via MATLAB", *International Journal of Applied Science and Technology*, Vol. 2, No. 8, 2012.

[21]Chopra, A. K., *Dynamics of Structures: Theory and Applications to Earthquake Engineering*, Prentice Hall, Englewood Cliffs, New Jersey, 1995.

[22]Marwala, T., *Finite-element-model updating using computational intelligence technique*, Springer-Verlag, London, 2010.

[23]Friswell, M. I., and Mottershead, J. E., *Finite Element Model Updating in Structural Dynamics*, Kluwer Academics, Dordrecht, The Netherlands.

[24]Price, K. V., Rainer, M. S., and Lampinen, J. A., *Differential Evolution: A Practical Approach to Global Optimization*, Springer-Verlag, Berlin, 2005.

[25]Markus, B., "Differential Evolution", *http://www.mathworks.com/matlabcentral/fileexchange/18593-differential-evolution*.